Platelet proteomic profiling reveals potential mediators of immunothrombosis and proteostasis in patients with myeloproliferative neoplasms

List of Supplementary Material:
- Methods
- Tables S1-S2 and legends
- Table S3-S13 legends
- Figure S1-S2 and legends

Methods

Study recruitment and sample preparation for platelet proteomics

Ethical approval was granted from the Institutional Review Board (IRB) of Papa Giovanni XXIII Hospital, Bergamo, Italy (IRB approval number 1789/2013) and the Mater Misericordiae University Hospital, Dublin, Ireland (IRB approval number 1/378/2241). Patients over the age of 18 with an established diagnosis of MPN (PV n= 41, ET n= 59) according to the World Health Organization classification criteria (in situ at time of diagnosis)[1, 2, 3] were invited to participate at their routine haematological follow-up (2014-2022). A control group of healthy donors (n= 40) were recruited from the same clinical sites and consisted of volunteers (predominantly hospital staff) over the age of 40, with no recent history of illness, no chronic inflammatory/medical conditions and not taking antiplatelet or anticoagulant therapy. Full blood count was assessed at the time of blood draw. Controls were not routinely screened for MPN driver mutations. Following informed consent, samples of whole blood collected in sodium citrate (0.105mol/L) were obtained by direct venipuncture. Platelets were isolated from platelet rich plasma (PRP) obtained by centrifugation of whole blood for 10 minutes at 400 *g* at room temperature (RT), according to an established previously published method[4]. Briefly, PRP was diluted in 1:2 ratio with Krebs Ringer buffer (4mM KCl, 107 mM NaCl, 20 mM $NaHCo_3$, 2mM Na_2SO_4, pH 5). After centrifugation at 1,000 *g* for 10 min at RT, the platelet pellet was resuspended

in Krebs Ringer buffer supplemented with glucose (0.9 g/L, PH 6) and centrifuged a second time (1,000 *g*, 10 min, RT). This washing procedure was repeated twice, and the platelets were resuspended at a concentration of 1x 10^9 platelets/mL in phosphate buffered saline (PBS) or PBS containing 1% Triton, snap frozen on dry ice and stored at -80 °C.

Mass Spectrometry

Platelets were lysed in RIPA buffer (100 mM Tris pH 8.0, 300 mM NaCl, 2% Triton-X 100, 0.2% SDS, 1% sodium deoxycholate) with protease and phosphatase inhibitors (Roche). Samples were precipitated with 95% acetone overnight at -20 °C, centrifuged at 14,000 *g* at 4 °C for 10 minutes and the supernatant was removed. The protein pellet was resuspended in PBS and protein concentration was estimated by measuring absorbance at 280nm using a DS-11 spectrophotometer (DeNovix) as before[5, 6]. Mass spectrometry sample preparation was performed using the commercially available PreOmics iST HT 192x kit (P.O.00067). In brief, 50 µg of protein was simultaneously lysed, reduced, and alkylated for 10 min at 95 °C and 1000 rpm, transferred to a cartridge and subsequently double-digested with LysC and trypsin at 37 °C and 500 rpm for 1 hour. Peptides were purified with repeated washes and eluted. Samples were evaporated at 45 °C and peptides resuspended in LC-load buffer. Digested peptides were loaded onto C18 trap columns (Evotip) and washed with 20 µL 0.1% formic acid (FA) followed by the addition of 100 µL storage solvent (0.1% FA). Differential proteomic signatures were established using liquid chromatography mass spectrometry (LC-MS) with a Bruker TimsTOF mass spectrometer connected to an EvoSep liquid chromatography system operated by the UCD Conway Proteomics Core facility.

Samples were loaded onto the Evosep One LC system and separated with an increasing acetonitrile gradient over 40 minutes at a flow rate of 250 nl/min at room temperature. The mass spectrometer was operated in positive ion mode with a capillary voltage of 1500V, dry gas flow of 3 l/min and a dry temperature of 180 °C. All data was acquired with the

instrument operating in trapped ion mobility spectrometry (TIMS) mode. Trapped ions were selected for MS/MS using parallel accumulation serial fragmentation (PASEF).

Identified peptides from platelet samples were searched against a human FASTA (July 2022) using MaxQuant (2.0.3.0) with specific parameters for trapped ion mobility spectra data dependent acquisition (TIMS DDA). In the main Andromeda search precursor, mass and fragment mass had an initial mass tolerance of 6 ppm and 20 ppm, respectively. The search included fixed modification of carbamidomethyl cysteine. Minimal peptide length was set to seven amino acids, and a maximum of two miscleavages was allowed. The false discovery rate (FDR) was set to 0.01 for peptide and protein identifications. The normalized protein intensity of each identified protein was used for label free quantitation (LFQ) as previously described[7].

Data analyses

Continuous data were summarized as medians and IQRs and categorical data are presented as frequencies and percentages. To compare differences in clinical variables between healthy controls and MPN subtypes (ET and PV), we used violin and box plots and conducted Mann-Whitney *U* test for non-parametric data. For unsupervised clustering and visualization, we performed principal component analyses (identifying MPN subtypes by color). All analyses were performed using the R studio interface (version 2023.03.1+446). Statistical analysis of the LFQ intensities was performed using Perseus (version 2.0.10) and R (version 4.3.1). Protein identifications were filtered to eliminate identifications from the reverse database, proteins only identified by site, and common contaminants. For downstream analysis, only proteins identified in at least 50% of samples in at least one group (control/ET/PV) were included. Missing values were imputed using the random forest method (Missforest package, R/Bioconductor). Data was log2-transformed and differential protein expression was established using the Limma software package within R/Bioconductor.

Differential protein expression was adjusted for batch, patient age, sex, and treatment (antiplatelet and cytoreductive therapy) as potential confounding variables within the linear model in Limma (design <- model.matrix(~patientvar$Subtype+patientvar$Batch+patientvar$Age+patientvar$Sex+patientvar$ASAnum+patientvar$HYDnum). Controlling for multiple comparisons was performed using the Benjamini-Hochberg defined false discovery rate (FDR). Significant differential protein expression was pre-specified as proteins with an FDR < 0.05 and a fold change of 1.5 in MPN, as compared to healthy controls.

A heatmap of the top 10 differentially expressed proteins (based on fold change and FDR <0.01) was generated using the pheatmap R package, and its built-in functions for hierarchical cluster analysis on the sample-to-sample Euclidean distance matrix of the expression data.

Proteomic quality control and validation analysis

To assess intra-donor platelet proteomic reproducibility, 6 patient samples were analyzed as technical replicates (5 in duplicate, 1 in triplicate). Pearson correlation coefficient (*r*) was performed on the log2 transformed LFQ- intensity of all proteins quantified (n= 1771) across technical replicate samples (**Figure S1**). To assess biological (inter-donor) variability in protein abundances, Pearson correlation coefficient (*r*) was performed on the log2 transformed LFQ-intensity of all proteins quantified (n= 1952) across biologic replicate samples (control n= 40; MPN n= 100) (**Figure S2**, **Tables S12** & **S13**).

Pathway/Gene set enrichment analysis for differentially expressed (DE) proteins.

Gene set enrichment analysis (GSEA)[8], a well-established method for determining regulatory patterns in co-expressed genes, was performed on the entire DE protein set for

each MPN subtype (PV & ET), using the Cancer Hallmarks gene sets from MSigDB[9]. The 'GSEA Pre-ranked' function was used with a metric score that combines fold change and adjusted p-value together for improved gene ranking. We used default settings with 1,000 gene set permutations to generate *p* and *q* values and compared MPN subtypes. In these analyses, to allow for a broad comparison, we assessed all proteins that were differentially expressed according to FDR/adjusted p < 0.25 as recommended by the authors of GSEA[8].

Supplementary Tables

Table S1: Characteristics of MPN Patients & Controls

	ET	**PV**	**Control**
Subject Count, n	59	41	40
Sample Count, n	59	41	40
Median age, y (range)	61 (32-86)	63 (38-83)	45 (24-61)
Female, n (%)	32 (54)	22 (54)	24 (60)
Platelet count (X10^9/L), median (25% quartile, 75% quartile)	540 (422, 778)	465 (318, 638)	244 (220, 265)
White cell count (X10^9/L), median (25% quartile, 75% quartile)	6.9 (6, 8.1)	8.9 (7.6, 11.2)	6.5 (5.2, 8.4)
Hemoglobin (g/dL), median (25% quartile, 75% quartile)	14.1 (13.4, 15.3)	14.5 (13.4, 15.4)	14 (13.2. 14.4)
Hematocrit (%), median (25% quartile, 75% quartile)	41.7 (40.3, 45.1)	44.3 (42.2, 46.9)	40 (37, 43)
History of arterial thrombosis, n (%)	5 (8.5)	6 (14.6)	0 (0)
History of venous thromboembolism, n (%)	2 (3.4)	1 (2.4)	0 (0)
Median time from diagnosis, y (range)	7 (1-31)	4 (1-30)	NA
MPN driver mutation, n (%)			
JAK2 V617F	26 (44)	41 (100)	0 (0)
CALR	18 (31)	0 (0)	0 (0)
MPL	2 (3)	0 (0)	0 (0)
Triple Negative	12 (21)	0 (0)	0 (0)
Missing	1 (1)	0 (0)	0 (0)
Therapy, n (%)			
Aspirin & hydroxyurea	27 (46)	28 (68)	0 (0)
Aspirin only	20 (34)	12 (30)	0 (0)
Hydroxyurea only	4 (7)	0 (0)	0 (0)
JAK inhibitor	0 (0)	0 (0)	0 (0)
No treatment	8 (13)	1 (2)	40 (100)

Table S1: MPN patient and healthy control characteristics recruited across two sites (Papa Giovanni XXIII Hospital, Bergamo, Italy and Mater Misericordiae University Hospital, Dublin, Ireland) for proteomic analysis.

Table S2

Candidate protein (Gene name)	Platelet differential expression by MPN subtype Absolute fold change (direction of change)	Cellular function and relationship to procoagulant, proinflammatory, and profibrotic pathways in other published work.
MMP1	**PV:** 4.5 (increased) **ET:** 5.2 (increased)	MMP1, an interstitial collagenase, is known to cleave protease-activated receptor 1 (PAR1) and promote platelet activation and regulate thrombogenesis in vitro[10, 11, 12]. Furthermore, MMP1 mediates tumor invasion by compromising vascular barrier integrity and has been associated with inferior prognosis in solid organ malignancies[13, 14, 15].
FcγRIIA	**PV:** 2 (increased) **ET:** 2 (increased)	Unbalanced FcγRIIA-mediated platelet aggregation was previously reported to promote thrombosis[16].
SERPINH1	**PV:** 2 (increased)	There is evidence of decreased expression or ablation of this collagen binding, platelet adhesion protein in immobilized mammals as a thromboprotective mechanism[17, 18, 19].
LGALS1	**PV:** 6.7 (increased) **ET:** 4.7 (increased)	Galactin-1 is a beta-galactosidase binding protein which is reported to promote tumour cell proliferation and survival in haematological malignancies[20]. Recent data delineates the contribution of galactin-1 to disease severity in myelofibrosis and identified the protein as a potential drug target with disease modifying effects[21].
S100A6	**ET:** 2 (increased)	The S100 family of proteins is a major player in hematopoietic proliferation and recent work has identified proinflammatory/profibrotic roles for S100A6, S100A8, S100A9 in bone marrow, granulocytes, and plasma in MPN[21, 22, 23, 24, 25, 26].
PDIA6	**PV:** 1.7 (increased)	Protein disulfide isomerases (PDIs) are key mediators of platelet ER homeostasis and the relationship between PDIs, ER & oxidative stress, platelet activation and thrombosis has recently been elucidated[27, 28].
HPSE	**PV:** 1.8 (increased)	Heparanase cleaves heparan sulfate proteoglycans and participates in extracellular matrix remodeling. It has been shown to be increased in the plasma extracellular vesicles of patients with PV[29].

DIAPH1	**PV:** 1.9 (increased) **ET:** 1.8 (increased)	We find increased expression of protein diaphanous homolog-1 (DIAPH1) possibly suggesting altered megakaryopoiesis in peripherally circulating platelets in PV and ET. DIAPH regulates proplatelet formation via Rho-mediated actin polymerization and microtubule assembly[30].
RAB4A	**PV:** 3.7 (increased) **ET:** 2.3 (increased)	A Ras GTPase signaling protein which regulates platelet alpha granule release[31].
CD63	**PV: 2.6** (decreased)	Downregulation of CD63 has been associated with proliferation and metastasis in solid organ malignancy regulated by IL-6, IL-27 and STAT3 signaling[32].
CTSC	**PV:** 2 (increased)	Abundant Cathepsin C drives inflammation through macrophage activation via NF-κB signaling pathway[33].
VAMP8	**ET:** 1.7 (increased)	VAMP8 regulates platelet granule secretion and thrombosis *in vivo*[34].
EIF4G1	**PV:** 2.1 (increased) **ET:** 1.74 (increased)	EIF4G1 has been identified as a prognostic biomarker in breast cancer[35].
HSP90AB1	**ET:** 1.5 (increased)	We find increased expression of heat shock proteins in ET (HSP90AB1, TRAP1) and PV (HYOU1, HSPH1, DNAJA2). Heat shock protein 70 kDa and heat shock protein 90 kDa are two families of chaperone networks with integral roles in protein folding, degradation, trafficking, and maturation. They are known to promote oncogenesis by protecting a spectrum of cancer related proteins[36, 37, 38].
SLC25A2	**PV:** 1.9 (decreased)	SLC25A2 is decreased in PV (with SLC2A3 and SLC44A1 differentially expressed in ET). Solute membrane carrier proteins have been associated with venous thromboembolism in genome wide association studies and *in vivo* models[39, 40].
RAB32	**PV:** 2.1 (increased) **ET:** 1.6 (increased)	RAB32 is increased in ET (along with mitochondrial membrane protein TOMM22). Mitochondria are recognized as key regulators of platelet procoagulant function[41]. Loss of mitochondrial protein RAB32 is associated with dense granule storage pool disease Hermansky-Pudlak syndrome[42].
PSMD11	**PV:** 2 (increased) **ET:** 1.7 (increased)	We show evidence of dysregulated protein degradation pathways with upregulation of PSMD11 along with differential expression of lysosomal proteins (SORT1 and ATP6V) and other proteasomal subunits. This reflects the work of other groups who have shown that protein quality-control pathways may be important in the pathogenesis of MPN and other prothrombotic diseases and represent novel therapeutic targets[43, 44, 45].

Table S2: Select/representative candidate proteins that may variably influence the proinflammatory, pro-thrombotic, and profibrotic processes in MPNs. Fold change reflects relative quantification in MPN subtypes compared to healthy controls.

Table S3: 1952 proteins were quantified (LFQ intensity, see Methods) across PV, ET, and control platelet lysate samples.

Table S4: 1315 proteins taken forward for downstream analysis. Proteins filtered to remove contaminants, proteins identified by site only, or in reverse. Proteins included were quantified across all groups (PV, ET, and control) and were present in at least 50% of samples in at least one group (see Methods).

Table S5: Full list of 227 differentially expressed platelet proteins (Benjamini Hochberg false discovery rate <0.05) identified between ET and control samples.

Table S6: Full list of 166 differentially expressed platelet proteins (Benjamini Hochberg false discovery rate <0.05) identified between PV and control samples.

Table S7: Full list of 178 differentially expressed platelet proteins (Benjamini Hochberg false discovery rate <0.05) identified between PV and *JAK2* V617F positive ET samples.

Table S8: No significantly differentially expressed platelet proteins (Benjamini Hochberg false discovery rate <0.05) identified between *JAK2* V617F and *CALR* positive ET patients.

Table S9: Full list of 90 differentially expressed platelet proteins (Benjamini Hochberg false discovery rate <0.05) identified between triple-negative and mutation positive ET samples.

Table S10: Full data for all molecular pathways identified in platelet proteome of ET patient cohorts.

Table S11: Full data for all molecular pathways identified in platelet proteome of PV patient cohorts.

Table S12: Correlation matrix with Pearson correlation coefficient *(r*) of log2 transformed LFQ intensity from biologic replicates of control (n= 40) samples.

Table S13: Correlation matrix with Pearson correlation coefficient (*r*) of log2 transformed LFQ intensity from biologic replicates of MPN (PV n= 41; ET n= 59) samples.

Supplementary Figures

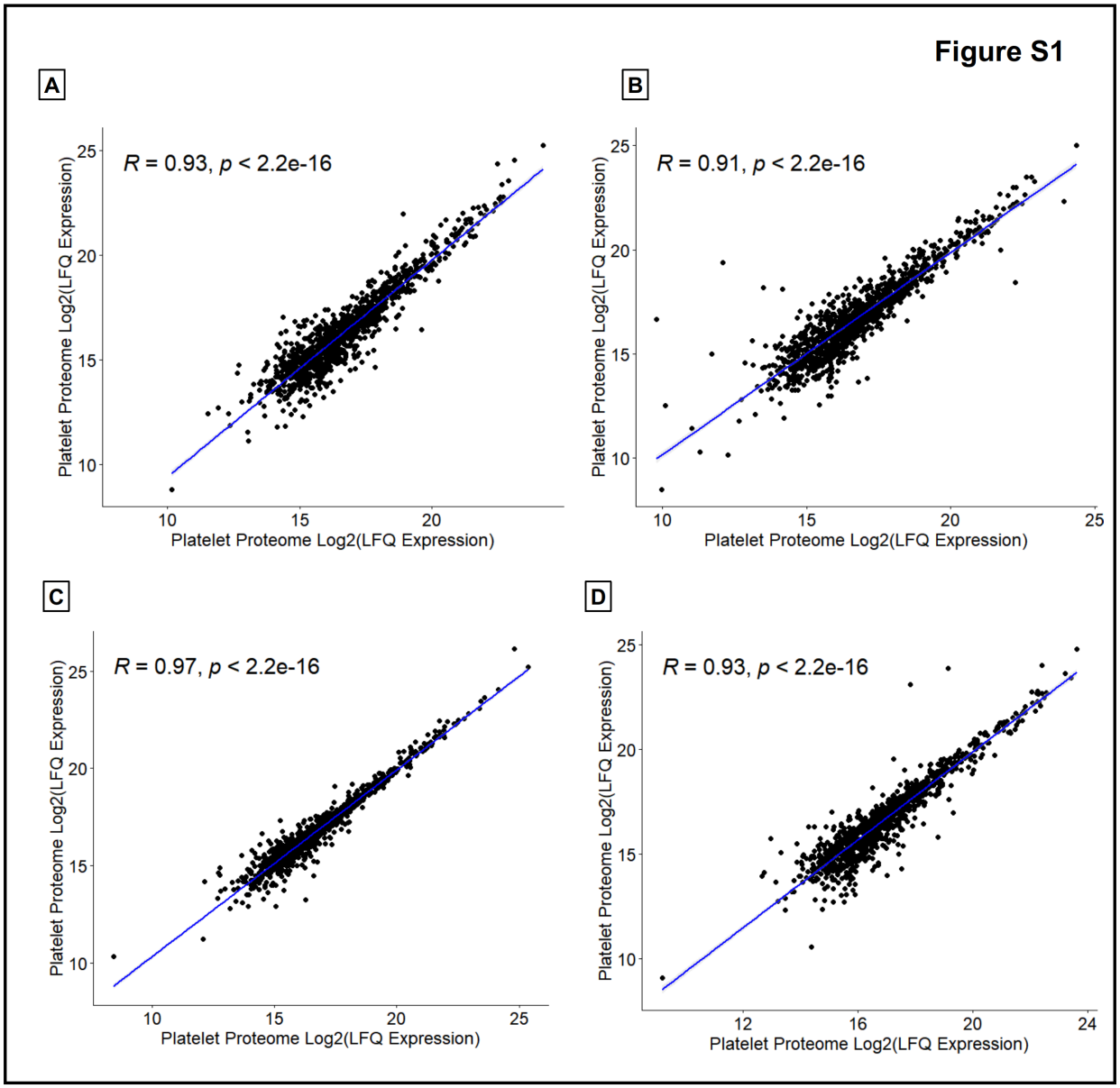

Figure S1: Strong correlation between platelet proteome technical replicates.
Pearson correlation coefficients (*r)* from representative samples **(A-D**) demonstrate intra-donor reproducibility with strong correlation of log transformed LFQ intensities from technical replicates of the platelet proteome.

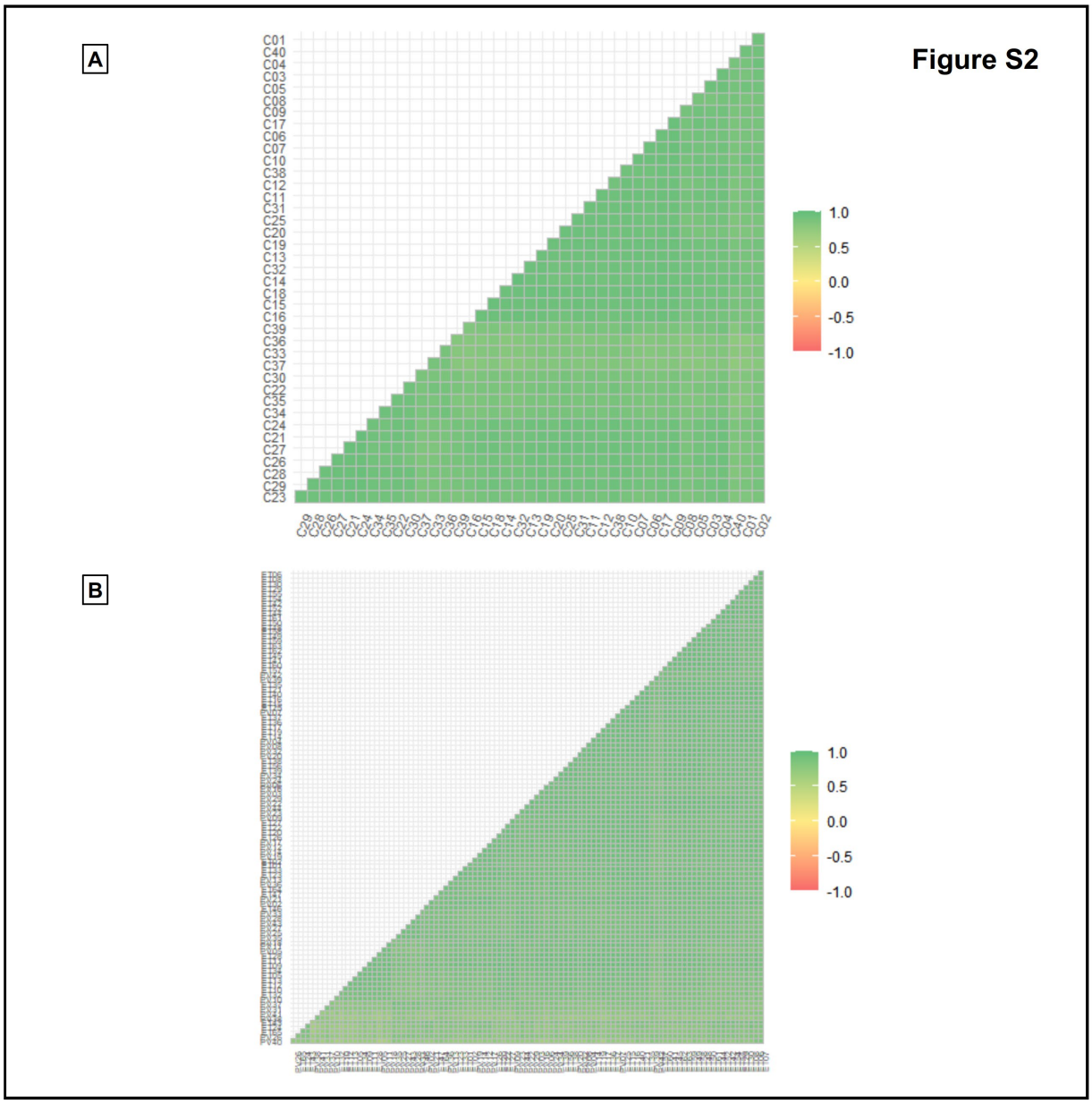

Figure S2: Strong correlation between platelet proteome biologic replicates

Correlation matrix of Pearson correlation coefficients (*r)* from biologic replicates show uniformly strong inter-donor reproducibility of the LFQ-proteomic analysis between biologic replicates from **(A)** controls (average $r = 0.90 \pm 0.04$, min $r = 0.75$, max $r = 0.97$) and **(B)** MPN (average $r = 0.88 \pm 0.06$, min $r = 0.57$, max $r = 0.98$) patient samples.

Bibliography

1. Jaffe E S. World Health Organization Classification of Tumours. Pathology & Genetics. Tumours of Hematopoietic and Lymphoid Tissues. IARC Press, Lyon. 2001.
2. Tefferi A, Vardiman JW. Classification and diagnosis of myeloproliferative neoplasms: the 2008 World Health Organization criteria and point-of-care diagnostic algorithms. Leukemia. 2008;22(1):14-22.
3. Arber DA, Orazi A, Hasserjian R, Thiele J, Borowitz MJ, Le Beau MM, et al. The 2016 revision to the World Health Organization classification of myeloid neoplasms and acute leukemia. Blood. 2016;127(20):2391-405.
4. Cortelazzo S, Marchetti M, Orlando E, Falanga A, Barbui T, Buchanan MR. Aspirin increases the bleeding side effects in essential thrombocythemia independent of the cyclooxygenase pathway: role of the lipoxygenase pathway. Am J Hematol. 1998;57(4):277-82.
5. Parsons MEM, Szklanna PB, Guerrero JA, Wynne K, Dervin F, O'Connell K, et al. Platelet Releasate Proteome Profiling Reveals a Core Set of Proteins with Low Variance between Healthy Adults. Proteomics. 2018;18(15):e1800219.
6. Szklanna PB, Parsons ME, Wynne K, O'Connor H, Egan K, Allen S, et al. The Platelet Releasate is Altered in Human Pregnancy. Proteomics Clin Appl. 2019;13(3):e1800162.
7. Weiss L, Keaney J, Szklanna PB, Prendiville T, Uhrig W, Wynne K, et al. Nonvalvular atrial fibrillation patients anticoagulated with rivaroxaban compared with warfarin exhibit reduced circulating extracellular vesicles with attenuated pro-inflammatory protein signatures. J Thromb Haemost. 2021;19(10):2583-95.
8. Subramanian A, Tamayo P, Mootha VK, Mukherjee S, Ebert BL, Gillette MA, et al. Gene set enrichment analysis: a knowledge-based approach for interpreting genome-wide expression profiles. Proc Natl Acad Sci U S A. 2005;102(43):15545-50.
9. Liberzon A, Birger C, Thorvaldsdóttir H, Ghandi M, Mesirov JP, Tamayo P. The Molecular Signatures Database (MSigDB) hallmark gene set collection. Cell Syst. 2015;1(6):417-25.
10. Austin KM, Covic L, Kuliopulos A. Matrix metalloproteases and PAR1 activation. Blood. 2013;121(3):431-9.
11. Trivedi V, Boire A, Tchernychev B, Kaneider NC, Leger AJ, O'Callaghan K, et al. Platelet matrix metalloprotease-1 mediates thrombogenesis by activating PAR1 at a cryptic ligand site. Cell. 2009;137(2):332-43.
12. Mastenbroek TG, Feijge MA, Kremers RM, van den Bosch MT, Swieringa F, De Groef L, et al. Platelet-Associated Matrix Metalloproteinases Regulate Thrombus Formation and Exert Local Collagenolytic Activity. Arterioscler Thromb Vasc Biol. 2015;35(12):2554-61.
13. Brinckerhoff CE, Rutter JL, Benbow U. Interstitial collagenases as markers of tumor progression. Clin Cancer Res. 2000;6(12):4823-30.
14. Nguyen CH, Senfter D, Basilio J, Holzner S, Stadler S, Krieger S, et al. NF-κB contributes to MMP1 expression in breast cancer spheroids causing paracrine PAR1 activation and disintegrations in the lymph endothelial barrier in vitro. Oncotarget. 2015;6(36):39262-75.
15. Boire A, Covic L, Agarwal A, Jacques S, Sherifi S, Kuliopulos A. PAR1 is a matrix metalloprotease-1 receptor that promotes invasion and tumorigenesis of breast cancer cells. Cell. 2005;120(3):303-13.

16. Arman M, Krauel K. Human platelet IgG Fc receptor FcγRIIA in immunity and thrombosis. J Thromb Haemost. 2015;13(6):893-908.
17. Thienel M, Müller-Reif JB, Zhang Z, Ehreiser V, Huth J, Shchurovska K, et al. Immobility-associated thromboprotection is conserved across mammalian species from bear to human. Science. 2023;380(6641):178-87.
18. Kaiser WJ, Holbrook LM, Tucker KL, Stanley RG, Gibbins JM. A functional proteomic method for the enrichment of peripheral membrane proteins reveals the collagen binding protein Hsp47 is exposed on the surface of activated human platelets. J Proteome Res. 2009;8(6):2903-14.
19. Sasikumar P, AlOuda KS, Kaiser WJ, Holbrook LM, Kriek N, Unsworth AJ, et al. The chaperone protein HSP47: a platelet collagen binding protein that contributes to thrombosis and hemostasis. J Thromb Haemost. 2018;16(5):946-59.
20. Giordano M, Croci DO, Rabinovich GA. Galectins in hematological malignancies. Curr Opin Hematol. 2013;20(4):327-35.
21. Li R, Colombo M, Wang G, Rodriguez-Romera A, O'Sullivan J, Clark S-A, et al. A pro-inflammatory stem cell niche drives myelofibrosis through a targetable galectin 1 axis. bioRxiv. 2023:2023.08.05.550630.
22. Diklić M, Mitrović-Ajtić O, Subotički T, Djikić D, Kovačić M, Bjelica S, et al. IL6 inhibition of inflammatory S100A8/9 proteins is NF-κB mediated in essential thrombocythemia. Cell Biochem Funct. 2020;38(4):362-72.
23. Leimkühler NB, Costa IG, Schneider RK. From cell to cell: Identification of actionable targets in bone marrow fibrosis using single-cell technologies. Exp Hematol. 2021;104:48-54.
24. Wang S, Song R, Wang Z, Jing Z, Wang S, Ma J. S100A8/A9 in Inflammation. Front Immunol. 2018;9:1298.
25. Wang YH, Chen YJ, Lai YH, Wang MC, Chen YY, Wu YY, et al. Mutation-Driven S100A8 Overexpression Confers Aberrant Phenotypes in Type 1 CALR-Mutated MPN. Int J Mol Sci. 2023;24(10).
26. Kovačić M, Mitrović-Ajtić O, Beleslin-Čokić B, Djikić D, Subotički T, Diklić M, et al. TLR4 and RAGE conversely mediate pro-inflammatory S100A8/9-mediated inhibition of proliferation-linked signaling in myeloproliferative neoplasms. Cell Oncol (Dordr). 2018;41(5):541-53.
27. Lay AJ, Dupuy A, Hagimola L, Tieng J, Larance M, Zhang Y, et al. Endoplasmic reticulum protein 5 attenuates platelet endoplasmic reticulum stress and secretion in a mouse model. Blood Adv. 2023;7(9):1650-65.
28. Yang M, Chiu J, Scartelli C, Ponzar N, Patel S, Patel A, et al. Sulfenylation links oxidative stress to protein disulfide isomerase oxidase activity and thrombus formation. J Thromb Haemost. 2023;21(8):2137-50.
29. Fel A, Lewandowska AE, Petrides PE, Wiśniewski JR. Comparison of Proteome Composition of Serum Enriched in Extracellular Vesicles Isolated from Polycythemia Vera Patients and Healthy Controls. Proteomes. 2019;7(2).
30. Pan J, Lordier L, Meyran D, Rameau P, Lecluse Y, Kitchen-Goosen S, et al. The formin DIAPH1 (mDia1) regulates megakaryocyte proplatelet formation by remodeling the actin and microtubule cytoskeletons. Blood. 2014;124(26):3967-77.
31. Shirakawa R, Yoshioka A, Horiuchi H, Nishioka H, Tabuchi A, Kita T. Small GTPase Rab4 regulates Ca2+-induced alpha-granule secretion in platelets. J Biol Chem. 2000;275(43):33844-9.
32. Yu S, Chen J, Quan M, Li L, Li Y, Gao Y. CD63 negatively regulates hepatocellular carcinoma development through suppression of inflammatory cytokine-induced STAT3 activation. J Cell Mol Med. 2021;25(2):1024-34.

33. Alam S, Liu Q, Liu S, Liu Y, Zhang Y, Yang X, et al. Up-regulated cathepsin C induces macrophage M1 polarization through FAK-triggered p38 MAPK/NF-κB pathway. Exp Cell Res. 2019;382(2):111472.
34. Joshi S, Banerjee M, Zhang J, Kesaraju A, Pokrovskaya ID, Storrie B, et al. Alterations in platelet secretion differentially affect thrombosis and hemostasis. Blood Adv. 2018;2(17):2187-98.
35. Li K, Tan G, Zhang X, Lu W, Ren J, Si Y, et al. EIF4G1 Is a Potential Prognostic Biomarker of Breast Cancer. Biomolecules. 2022;12(12).
36. Albakova Z, Armeev GA, Kanevskiy LM, Kovalenko EI, Sapozhnikov AM. HSP70 Multi-Functionality in Cancer. Cells. 2020;9(3).
37. Trepel J, Mollapour M, Giaccone G, Neckers L. Targeting the dynamic HSP90 complex in cancer. Nat Rev Cancer. 2010;10(8):537-49.
38. Zhang J, Li H, Liu Y, Zhao K, Wei S, Sugarman ET, et al. Targeting HSP90 as a Novel Therapy for Cancer: Mechanistic Insights and Translational Relevance. Cells. 2022;11(18).
39. Bennett JA, Mastrangelo MA, Ture SK, Smith CO, Loelius SG, Berg RA, et al. The choline transporter Slc44a2 controls platelet activation and thrombosis by regulating mitochondrial function. Nat Commun. 2020;11(1):3479.
40. Germain M, Chasman DI, de Haan H, Tang W, Lindström S, Weng LC, et al. Meta-analysis of 65,734 individuals identifies TSPAN15 and SLC44A2 as two susceptibility loci for venous thromboembolism. Am J Hum Genet. 2015;96(4):532-42.
41. Ajanel A, Campbell RA, Denorme F. Platelet mitochondria: the mighty few. Curr Opin Hematol. 2023;30(5):167-74.
42. Aguilar A, Weber J, Boscher J, Freund M, Ziessel C, Eckly A, et al. Combined deficiency of RAB32 and RAB38 in the mouse mimics Hermansky-Pudlak syndrome and critically impairs thrombosis. Blood Adv. 2019;3(15):2368-80.
43. Osorio FG, Soria-Valles C, Santiago-Fernández O, Bernal T, Mittelbrunn M, Colado E, et al. Loss of the proteostasis factor AIRAPL causes myeloid transformation by deregulating IGF-1 signaling. Nat Med. 2016;22(1):91-6.
44. LaFave LM, Levine RL. Targeting a regulator of protein homeostasis in myeloproliferative neoplasms. Nat Med. 2016;22(1):20-1.
45. Jutzi JS, Marneth AE, Jiménez-Santos MJ, Hem J, Guerra-Moreno A, Rolles B, et al. CALR-mutated cells are vulnerable to combined inhibition of the proteasome and the endoplasmic reticulum stress response. Leukemia. 2023;37(2):359-69.